


Key Points:

- The magnetosheath flow angle to the local magnetopause normal vector is associated with the magnetic shear angle
- The reconnection electric field is inversely proportional to the solar wind-Alfvén Mach number
- The reconnection outflow speed is proportional to the solar wind-Alfvén speed

Correspondence to:

D. Koga,
 dkaqua@kyudai.jp

Citation:

Koga, D., Gonzalez, W. D., Souza, V. M., Cardoso, F. R., Wang, C., & Liu, Z. K. (2019). Dayside magnetopause reconnection: Its dependence on solar wind and magnetosheath conditions. *Journal of Geophysical Research: Space Physics*, 124. <https://doi.org/10.1029/2019JA026889>

Received 25 APR 2019

Accepted 9 OCT 2019

Accepted article online 14 NOV 2019

Dayside Magnetopause Reconnection: Its Dependence on Solar Wind and Magnetosheath Conditions

D. Koga^{1,2}, W. D. Gonzalez^{1,2}, V. M. Souza¹, F. R. Cardoso³, C. Wang², and Z. K. Liu^{1,2}

¹National Institute for Space Research - INPE, São José dos Campos, Brazil, ²State Key Laboratory of Space Weather, National Space Science Center, Chinese Academy of Sciences, Beijing, China, ³School of Engineering - EEL, University of São Paulo, Lorena, Brazil

Abstract Magnetic reconnection permits topological rearrangements of the interplanetary and magnetospheric magnetic fields and the entry of solar wind mass, energy, and momentum into the magnetosphere. Thus, magnetic reconnection is a key issue to understand space weather. However, it has not been fully understood yet under which interplanetary/magnetosheath conditions magnetic reconnection takes place more effectively at the dayside magnetopause. In the present study 25 dayside magnetopause reconnection events are investigated using the “Time History of Events and Macroscale Interactions during Substorms” (THEMIS) satellite observations in order to find its dependence on solar wind and magnetosheath conditions. It is found that the reconnection electric field is proportional to the interplanetary electric field and inversely proportional to the solar wind-Alfvén Mach number and that the reconnection outflow speed is proportional to the solar wind Alfvén speed and inversely proportional to the magnetosheath plasma beta. It is also shown that the range of magnetic shear angles for which magnetic reconnection should occur is restricted to large shears as the magnetosheath flow direction becomes more perpendicular to the direction of the local magnetopause normal vector. Since these results refer to fairly typical solar wind-Alfvén Mach number condition, they may not necessarily apply to more extreme cases.

1. Introduction

Magnetic reconnection is a fundamental process for the mass, momentum, and energy transfer from the solar wind to Earth's magnetosphere. Since Dungey (1961) suggested the importance of magnetic reconnection for the solar wind-magnetosphere interaction, dayside reconnection events have been observed in situ at the Earth's dayside magnetopause (e.g., Deng & Matsumoto, 2001; Paschmann et al., 1979). Although recent reconnection studies have been dedicated to the microphysics of reconnection in the diffusion region, such as those involving data from the Magnetospheric Multiscale (MMS) mission (Burch et al., 2016), the macroscopic physics of reconnection still remains an important issue for understanding its large-scale features, which are of special interest for space weather predictions. In order to investigate the details of dayside reconnection processes from a macroscopic point of view, there have been several studies on the relationship between the solar wind/magnetosheath conditions and Earth's dayside reconnection. Paschmann et al. (1986) found that the occurrence of high-speed outflows near the reconnection site, which is a proxy of dayside reconnection, is inversely correlated with the magnetosheath plasma beta β , the ratio of the plasma pressure to the magnetic pressure, with reconnection less likely to occur when $\beta > 2$. Scully et al. (1994a, 1994b) showed how the upstream solar wind parameters control reconnection using a geomagnetic activity index as a proxy measure of the efficiency of dayside reconnection. They showed that the solar wind-magnetosonic Mach number, upstream solar wind plasma beta, and the cone angle of the interplanetary magnetic field (IMF) are correlated with such a proxy measure of the efficiency of the reconnection process. Each of these three parameters controls the plasma beta in the magnetosheath downstream of the Earth's bow shock. The dependence of the efficiency of reconnection on the above parameters is in agreement with the expectation that large magnetosheath betas reduce the rate of or hinder the onset of dayside reconnection. Phan, Paschmann, et al. (2013) found that for low $\Delta\beta$ (the difference in the plasma beta on the two sides of the magnetopause), the majority of reconnection events occurred over a large range of magnetic shears, whereas when $\Delta\beta$ was high reconnection events occurred only for high magnetic shears.

©2019. The Authors.

This is an open access article under the terms of the Creative Commons Attribution-NonCommercial-NoDerivs License, which permits use and distribution in any medium, provided the original work is properly cited, the use is non-commercial and no modifications or adaptations are made.

Table 1
The 25 Magnetopause Reconnection Events

No.	Reference	Date	Time (UT)	Probe	X (R_E)	Y (R_E)	Z (R_E)
1	Dunlop et al. (2011)	2007/06/14	04:42	A	9.72	2.82	-2.22
2	Trattner et al. (2012)	2007/06/23	06:50	C	10.28	1.49	-2.76
3	Trattner et al. (2012)	2007/06/28	12:40	E	10.65	0.63	-2.96
4	Mozer et al. (2008)	2007/07/20	17:38	C	11.08	-2.47	-2.72
5	Trattner et al. (2012)	2007/07/22	02:20	C	12.04	-1.98	-3.21
6	Hietala et al. (2018)	2007/08/07	22:59	B	9.58	-5.29	-2.45
7	Zhang et al. (2012)	2007/08/26	08:32	C	9.93	-8.27	0.41
8	Trattner et al. (2012)	2007/08/28	08:20	C	10.08	-1.88	-2.00
9	Trattner et al. (2012)	2008/07/27	20:15	E	9.67	4.66	-3.51
10	Phan, Paschmann, et al. (2013)	2008/07/30	19:33	D	9.87	4.83	-3.49
11	Sonnerup et al. (2016)	2008/08/03	17:00	D	10.00	2.08	-3.77
12	Teh et al. (2010)	2008/08/06	21:14	E	10.31	4.12	-3.31
13	Phan, Shay, et al. (2013)	2008/08/09	15:13	D	9.63	-0.22	-3.25
14	Trattner et al. (2012)	2008/08/31	15:09	D	10.33	-2.64	-2.01
15	Phan et al. (2016)	2008/09/09	21:45	D	10.77	0.88	-1.66
16	Walsh et al. (2014)	2008/09/15	13:34	D	9.25	-5.02	-0.46
17	Souza et al. (2017)	2009/05/22	16:24	B	7.31	8.75	-0.46
18	Souza et al. (2017)	2009/07/07	14:39	C	9.09	2.81	-3.06
19	Tang et al. (2013)	2009/08/27	15:35	E	8.79	0.72	-2.29
20	Mozer et al. (2011)	2009/08/30	14:41	D	9.04	0.46	-2.09
21	Pritchett et al. (2012)	2010/09/08	16:05	D	8.51	4.44	-1.09
22	Uchino et al. (2017)	2011/11/22	15:00	D	8.59	-1.19	3.45
23	Dai et al. (2015)	2013/02/13	23:25	E	6.15	-6.88	-0.61
24	Walsh et al. (2017)	2014/04/21	11:55	A	9.61	-3.04	-1.67
25	Zou et al. (2018)	2014/05/23	15:51	A	5.24	-9.84	-2.05

Furthermore, nonreconnection events occurred primarily in the $\Delta\beta$ -shear regime in which reconnection is predicted to be suppressed, in good agreement with the theory (Swisdak et al., 2003, 2010).

In the present study 25 dayside magnetopause reconnection events are investigated in order to find its dependence on solar wind and magnetosheath conditions.

2. Data

The “Time History of Events and Macroscale Interactions during Substorms” (THEMIS) satellites were launched in 2007 to determine the onset mechanism and macroscale evolution of substorms (Angelopoulos, 2008). Observational data used in the present study are particle data from the Electrostatic Analyzer (ESA; McFadden et al., 2008) and magnetic field data from the Fluxgate Magnetometer (FGM; Auster et al., 2008). The THEMIS ion and electron electrostatic analyzers (iESA and eESA) measure plasma over the energy range from a few eV up to 30 keV for electrons and up to 25 keV for ions each 3-s spin period. The FGM instrument measures the magnetic field from DC up to 64 Hz in the near-Earth space. Here, we used magnetic field data with a 3-s spin resolution. The magnetosheath and magnetospheric parameters associated with dayside magnetopause reconnection were calculated as a 15-s average value (to include at least five data points) for both sides of the magnetopause transition region.

The solar wind particle and the IMF data were obtained from the NASA OMNI database (King & Papitashvili, 2005). These are time shifted to take into account the solar wind convection time from the spacecraft position to the bow shock nose. For solar wind parameters, the 5-min preceding values for each reconnection event were used, considering the solar wind propagation from the bow shock nose to the magnetopause. The geocentric solar magnetospheric (GSM) coordinate system was used for all quantities in the present

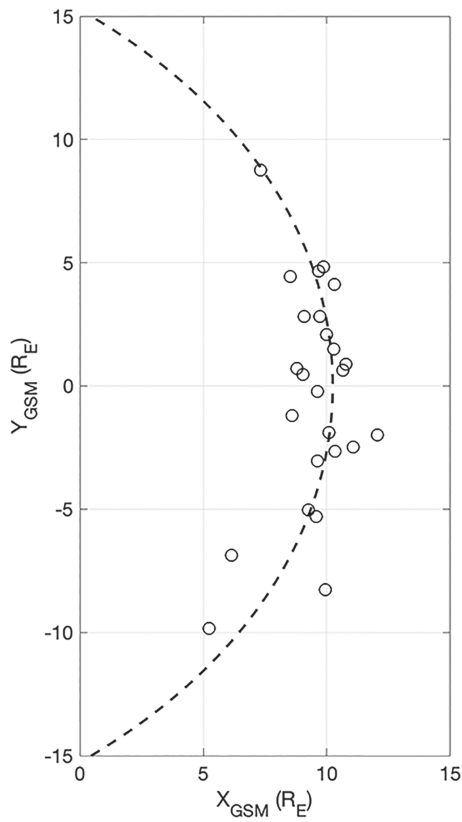


Figure 1. The GSM X-Y plane position for the selected magnetopause reconnection events observed by THEMIS from 2007 to 2014. The dotted curve indicates the nominal position of the magnetopause (Shue et al., 1998), considering an IMF B_z component of 2.0 nT and a solar wind dynamic pressure of 2.0 nPa.

study, except for the flow velocity and magnetic field in sections 3.3 and 4, which are in the LMN boundary coordinate system where \mathbf{N} is normal to the boundary, \mathbf{M} is tangential to the boundary and positive pointing toward dawn, and $\mathbf{L} = \mathbf{M} \times \mathbf{N}$. The GSM to LMN transformation was done using Shue's empirical magnetopause model (Shue et al., 1998).

Since 2007, THEMIS probes have been crossing the magnetopause many times from the dusk to the dawn flank. In the present study, we investigate 25 dayside magnetic reconnection events as listed in Table 1. These magnetic reconnection events have been reported by several authors (see references in Table 1).

3. Results

The 25 reconnection events have been selected near the dayside magnetopause. Figure 1 shows satellite positions in the GSM X-Y plane for the 25 magnetopause reconnection events where the dotted curve indicates the nominal position of the magnetopause (Shue et al., 1998), considering an IMF B_z component of 2.0 nT and a solar wind dynamic pressure of 2.0 nPa. The events are distributed almost uniformly from $Y = -10 R_E$ to $Y = 10 R_E$ ($R_E = 6,371$ km).

3.1. Magnetic Shear Angle

First of all, we investigate the magnetic shear properties of the reconnection region in the 25 events associated with the observed solar wind and magnetosheath conditions. In Figure 2, the magnetic shear angle between the magnetosheath and magnetospheric magnetic fields is shown, as a function of the solar wind flow pressure (left) and the difference in the plasma beta between both sides of the magnetopause (right). Figure 2a shows that the magnetic shear angle gets limited to high angles as the solar wind flow pressure increases. The same behavior is also observed for other solar wind parameters such as the solar wind speed and number density (not shown).

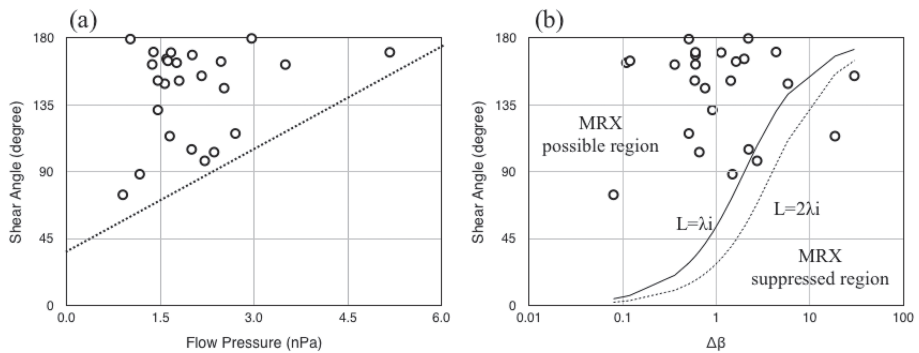


Figure 2. The magnetic shear angle between the magnetosheath and magnetospheric magnetic fields as a function of the solar wind flow pressure (left) and of the difference of plasma beta between both sides of the magnetopause (right).

Using observational data acquired at the Earth's dayside magnetopause, Phan, Paschmann, et al. (2013) found that the magnetic shear angle θ associated with magnetic reconnection is limited to high values for high $\Delta\beta$. They suggested the following:

$$\Delta\beta > \frac{2L}{\lambda_i} \tan(\theta/2), \quad (1)$$

where L represents a typical pressure gradient scale near the X-line and λ_i is the ion inertial length. The inequality is based on a theoretical consideration in which diamagnetic drifts suppress the magnetic reconnection when the X-line convection speed v^* is larger than the Alfvén speed V_A , $v^* > V_A$ (Swisdak et al., 2003, 2010). In the present study, most of the magnetic reconnection events are also found at the possible reconnection (MRX) region as shown in Figure 2b. The solid and dotted curves denote two different values of pressure gradient scale: $L = \lambda_i$ and $L = 2\lambda_i$, respectively.

3.2. Reconnection Outflow Speed

Next, we investigate the dependence of the reconnection outflow speed on some solar wind and magnetosheath parameters. The observed outflow velocity is obtained by the following expression,

$$\mathbf{V}_o(\text{observation}) = \mathbf{V}_{max} - \mathbf{V}_{background} \quad [\text{km/s}], \quad (2)$$

where \mathbf{V}_{max} is the maximum velocity during the magnetopause crossing and $\mathbf{V}_{background}$ is the background magnetosheath velocity. On the other hand, the theoretical outflow speed was calculated using the Cassak and Shay (2007) model, which is for asymmetric magnetic reconnection and is well cited and used, that is,

$$n_o = \frac{n_1 B_2 + n_2 B_1}{B_1 + B_2} \quad [\text{cm}^{-3}], \quad (3)$$

$$V_o(\text{theory}) = 0.218 \times 10^2 \sqrt{\frac{B_1 B_2}{n_o}} \quad [\text{km/s}], \quad (4)$$

where the subscripts 1 and 2 denote the magnetosheath and magnetospheric sides of the magnetopause, respectively, and the magnetic field intensity is in nT and the ion density n is in cm⁻³. We found that the observed reconnection outflow speed is proportional to the theoretical one as shown in Figure 3a. The reconnection outflow speed from theory increases as the solar wind bulk speed increases (Figure 3b) and decreases as the magnetosheath plasma beta β_{sh} increases (Figure 3c). In addition, the magnetosheath plasma beta dependence on the solar wind-Alfvén Mach number is shown in Figure 3d. When the solar wind-Alfvén Mach number M_A is high, the magnetosheath plasma beta is also high in the semilog plot.

Figure 4 shows the theoretical reconnection outflow speed (left) and the solar wind-Alfvén Mach number (right) associated with the solar wind Alfvén speed V_{Asw} . It is found that the theoretical reconnection outflow speed is proportional to the solar wind Alfvén speed. The solar wind-Alfvén Mach number decreases when the solar wind Alfvén speed increases due to $M_A = V_{sw}/V_{Asw}$.

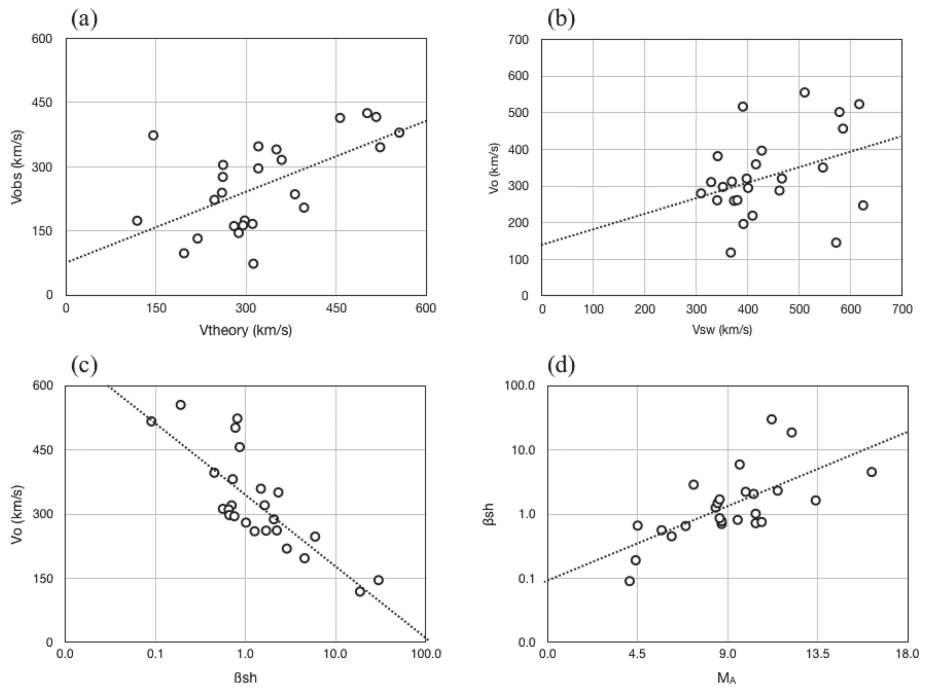


Figure 3. The reconnection outflow speed: (a) theory Cassak and Shay (2007) versus observation of the outflow speed, (b) the solar wind bulk speed versus the theoretical outflow speed, (c) the magnetosheath plasma beta versus the theoretical outflow speed, and (d) the solar wind-Alfvén Mach number versus magnetosheath plasma beta. The dotted lines in each panel are the linear or lognormal fitting.

3.3. Reconnection Electric Field

Third, we investigate the dependence of the reconnection electric field on the interplanetary electric field and the solar wind-Alfvén Mach number. The reconnection electric field intensity E_{rec} was calculated as

$$E_{\text{rec}} \propto |B_N \times V_L|, \quad (5)$$

where B_N is the normal component of the outflowing magnetic field and V_L is the L-component of the ion velocity of the observed reconnection outflow jet. As shown in Figure 5a, the reconnection electric field E_{rec} increases as the interplanetary electric field E_{IMF} increases, where E_{IMF} was calculated as $V_{\text{sw}} \sqrt{B_y^2 + B_z^2}$. On the other hand, E_{rec} decreases when the solar wind-Alfvén Mach number increases as shown in Figure 5b.

E_{rec} is also proportional to $V_o B_o$ where we define $B_o = \sqrt{B_1 B_2}$ (Cassak & Shay, 2007). Since there is no observational information on the aspect ratio of the diffusion region, we could not obtain a reasonable E_{rec} value. However, this relation will be discussed in section 4.

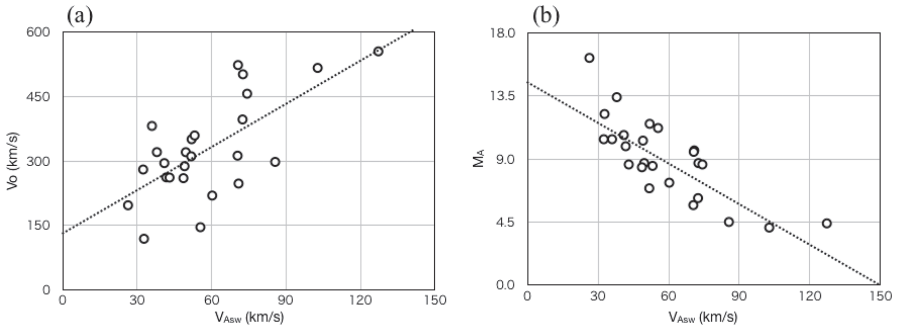


Figure 4. The theoretical reconnection outflow speed (left) and the solar wind-Alfvén Mach number (right) associated with the solar wind Alfvén speed V_{Asw} .

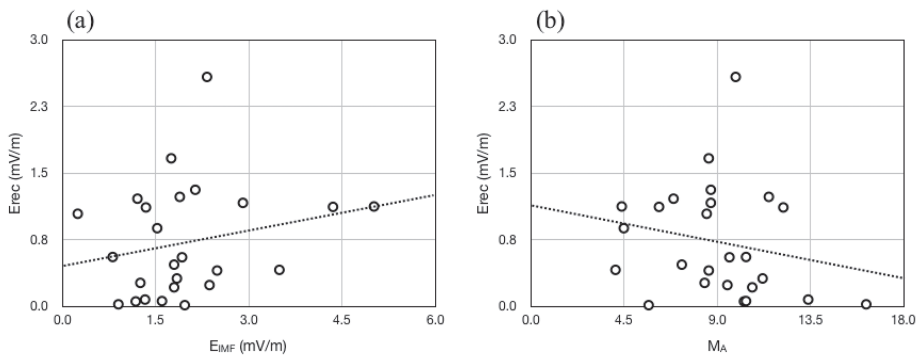


Figure 5. The reconnection electric field E_{rec} associated with the interplanetary electric field E_{IMF} (left) and the solar wind-Alfvén Mach number M_A (right).

4. Discussion and Conclusions

As seen in the previous section, reconnection-associated parameters, namely, magnetic shear angle θ , outflow speed V_o , and electric field E_{rec} , are affected by several properties of the solar wind and the magnetosheath. The results obtained from our investigation using 25 magnetopause reconnection events can be summarized as follows:

1. The reconnection magnetic shear is restricted to large shear values as the solar wind flow pressure and $\Delta\beta$ increase (Figure 2). This result is in agreement with the Phan, Paschmann, et al. (2013)'s suggestion.
2. V_o (observation) $\propto V_o$ (theory): The observed outflow speed is proportional to the expected theoretical value calculated using Cassak and Shay (2007) model (Figure 3a).
3. $V_o \propto V_{sw}$ ($V_o \propto V_{Asw}$): The reconnection outflow speed increases as the solar wind bulk (Alfvén) speed increases (Figures 3b and 4a). This relation was also confirmed in a frame comoving with the reconnecting current layer (not shown).
4. $\beta_{sh} \propto \exp(M_A)$: The magnetosheath plasma beta increases as the solar wind-Alfvén Mach number increases (Figure 3d). When the solar wind-Alfvén Mach number is large, the thermal pressure in the magnetosheath increases. Thus, plasma beta in the magnetosheath increases.
5. $V_o \propto -\log \beta_{sh}$: The reconnection outflow speed decreases as the magnetosheath plasma beta increases (Figure 3c). This supports the result suggested by Paschmann et al. (1986).
6. $E_{rec} \propto E_{IMF}$: The reconnection electric field is proportional to the interplanetary electric field (Figure 5a).
7. $E_{rec} \propto -M_A$ ($V_o \propto -M_A$): The reconnection electric field (or reconnection outflow speed) decreases as the solar wind-Alfvén Mach number increases (Figure 5b). The relation $V_o \propto -M_A$ can be obtained by substituting the expression mentioned in Finding 4 into that of Finding 5. This result is similar to Scurry et al. (1994b) observations.

From the findings, one could infer the following: When the solar-wind Alfvén speed V_{Asw} is large, one expects a small Alfvén Mach number M_A (Figure 4b). After the solar wind with small M_A crosses the bow shock, the solar wind plasma in the magnetosheath is less heated, and a small plasma beta β_{sh} is expected in the magnetosheath (or a small $\Delta\beta$). Also, a higher magnetosheath magnetic field intensity (a small β_{sh}) is expected, which in turn would generate a larger reconnection outflow speed V_o . Then, a large reconnection electric field E_{rec} is obtained, and reconnection would not be suppressed for a large range of magnetic shear angle. Thus, the present study can connect all the results reported in past studies as mentioned in section 1.

As for the solar wind electric field, we used a simple expression $V_{sw}\sqrt{B_y^2 + B_z^2}$ although there are various coupling functions, ranging from the simple $V_{sw}B_z$ to more complex functions such as that of Newell et al. (2007), Borovsky (2013), and Borovsky and Birn (2014). Borovsky and Birn (2014) showed that the reconnection rate starts to decouple from the solar wind electric field for $M_A < 4$. This is related to the issue of the saturation of the ionospheric potential, which implies saturation of the dayside merging rate for a large IMF (low Alfvén Mach number solar wind flow; Lopez et al., 2010). For the present reconnection events the range of M_A was from 4 to 16. Thus, our cases were still within the regime where the reconnection rate may not be influenced by saturation.

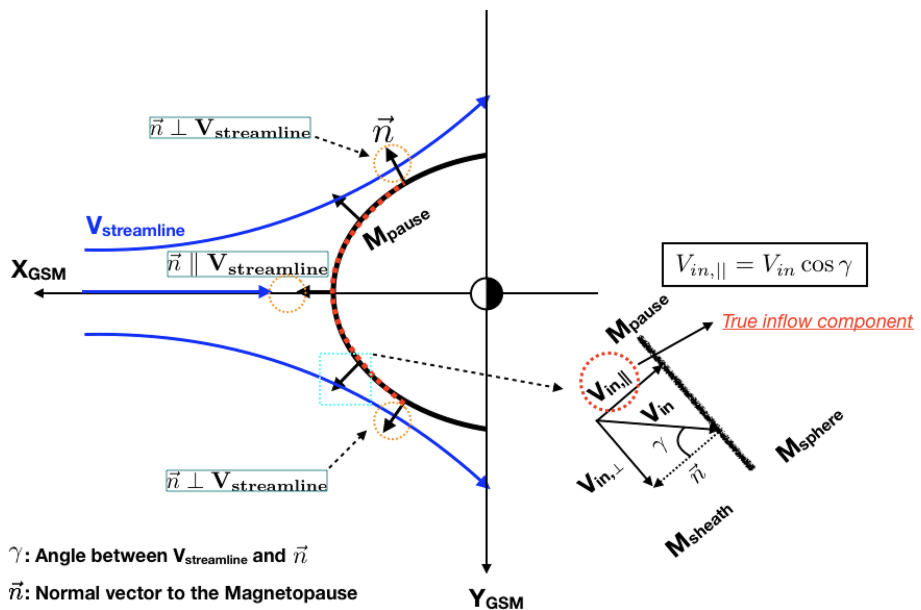


Figure 6. Schematic for the magnetosheath flow streamline around the magnetopause at the equatorial region ($Z_{GSM} = 0$).

V_{sw} is also proportional to the reconnection outflow speed V_o , but it is more difficult to find a clear causal relationship than that for V_{Asw} . Since V_{Asw} is a proxy for the IMF strength, the solar wind-Alfvén Mach number will scale like $1/B_{IMF}$. It should be noted here that although V_{Asw} also depends on the square root of the solar wind density, the influence on V_{Asw} was not significant, at least for the present study. Thus, Findings 3 and 7 are a consequence of the fact that for the range of Alfvén Mach numbers in the present investigation, the reconnection electric field is proportional to the solar wind electric field (Finding 6).

On a relation between solar wind flow pressure values and local magnetic shear angles, Figure 2a shows only that such a dependence exists, but we do not know if this behavior continues for a much larger data set.

It is interesting to analyze the influence of the magnetosheath shear flow on magnetopause reconnection occurrence. Figure 6 shows a schematic for the magnetosheath flow streamline around the magnetopause at the equatorial region ($Z_{GSM} = 0$). At the magnetopause nose, the streamline and normal direction to the magnetopause \vec{n} are antiparallel in the X-Y plane. At the dawn/dusk flank of the magnetopause, the angle γ between the streamline and magnetopause normal direction becomes close to 90° ($V_{in,\parallel}$ becomes small). Thus, the reconnection inflow speed normal to the magnetopause is reduced when one moves away from the magnetopause nose and the reconnection process ceases unless there exist plasma instabilities, such as the Kelvin-Helmholtz instability or pressure pulses (also known as jets; e.g., Shue et al., 2009), which could deform the magnetopause boundary shape. According to the THEMIS investigation done by Haaland et al. (2019), the magnetopause motion speed is higher at the dawn/dusk flank (~60 km/s) than that around the dayside (~20 km/s). Let us suppose, for the sake of argument, that the magnetosheath flow be zero. Then the relative inflow magnetosheath speed at the dawn/dusk flank would be much higher than that around the dayside. However, the magnetosheath flow direction around the dayside is quasi-parallel to the magnetopause normal direction while the flow direction is tangential at the dawn/dusk flank. Since the magnetosheath inflow speed is relative one between the magnetosheath flow and the magnetopause motion, the speed at the dawn/dusk flank would be comparatively smaller than or comparable to that around the dayside.

It should be noted here that there are several studies on magnetic reconnection with shear flows along the reconnecting magnetic fields (Cassak, 2011; Cassak & Otto, 2011; Doss et al., 2015; La Belle-Hamer et al., 1994; 1995; Tanaka et al., 2010), but the influence of perpendicular shear flows on magnetic reconnection has not been studied well for observational investigations although there have been some numerical studies (Liu et al., 2018; Ma et al., 2016). Ma et al. (2016) investigated the influence of such a perpendicular flow shear on magnetic reconnection and found using resistive MHD simulations that when the shear flow speed

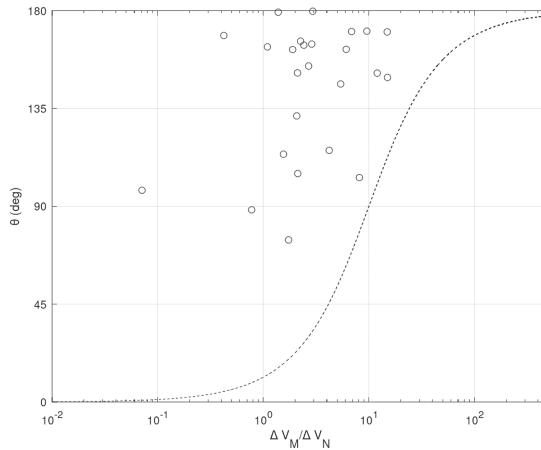


Figure 7. The magnetic shear angle θ as a function of the $\Delta V_M / \Delta V_N$ ratio. The dotted curve is calculated using equation (10) with $R = 0.1$.

$V_{in,\perp}$ (or V_M in the LMN boundary coordinate system) perpendicular to the reconnecting magnetic field lines is larger than the supercritical flow speed (the fast mode speed), an expanded density depletion layer in the outflow region is formed and is associated with an increase in the tangential magnetic field intensity $|B_M|$ in order to maintain total pressure balance (the boundary normal coordinate system is used here). They explained theoretically the result as follows: For a quasi one-dimensional layer for antiparallel magnetic reconnection (initially $B_M = 0$), the induction equation can be written as

$$\frac{\partial B_M}{\partial t} \sim B_N \frac{\partial V_M}{\partial N}. \quad (6)$$

Taking integration of the equation in time yields

$$B_M \sim B_N \frac{\partial V_M}{\partial N} \Delta t, \quad (7)$$

where Δt is the half-crossing time across the current layer. Equation (7) indicates that the normal magnetic field component B_N and the sheared flow perpendicular to the reconnection layer V_M (i.e., the magnetopause) generate magnetic field B_M flux in the outflow region due to the frozen-in condition.

Using this numerical result for our observations, it is investigated the influence of the magnetosheath flow on magnetic shear angle. Assuming $\partial V_M / \partial N \sim \Delta V_M / \Delta N$ where ΔN is the half-width of the current layer and ΔV_M is defined as the tangential magnetosheath flow speed, the above equation becomes

$$B_M \sim B_N \frac{\Delta V_M}{\Delta N / \Delta t}. \quad (8)$$

Then, dividing both sides of this equation by B_L , the following expression is obtained:

$$\frac{B_M}{B_L} \sim \frac{B_N}{B_L} \frac{\Delta V_M}{\Delta V_N}, \quad (9)$$

where ΔV_N is the normal magnetosheath flow speed defined as $\Delta N / \Delta t$. For the right-hand side of the equation, B_N / B_L is defined as the reconnection rate from the boundary condition for the tangential electric field $B_{in} B_L = B_{out} B_N$, since the traditional definition of the reconnection rate is $R \equiv V_{in} / V_{out}$ where V_{in} (V_{out}) is the reconnection inflow (outflow) speed. On the other hand, B_M / B_L refers to the magnetic shear across the current sheet, and we define it as $B_M / B_L \equiv \tan(\theta/2)$, as similarly done by Swisdak et al. (2010). Thus, equation (9) is rewritten as

$$\frac{\Delta V_M}{\Delta V_N} \sim \frac{1}{R} \tan \frac{\theta}{2}. \quad (10)$$

As shown in Figure 6 it is clear that ΔV_N (ΔV_M) is large (small) around the subsolar point of the magnetopause, while it becomes smaller (larger) at the dawn/dusk flank. The flow speeds ΔV_M and ΔV_N are a

function of the magnetopause position, and the magnetic shear angle is also a function of the magnetopause position.

Figure 7 shows the magnetic shear angle from the present observational data as a function of the $\Delta V_M / \Delta V_N$ ratio. The dotted curve in the figure is calculated using equation (10) where $R = 0.1$ was used as the reconnection rate from the theoretical and observational evidences (Cassak et al., 2017). The magnetic shear angle tends to be restricted to a large angle when $\Delta V_M / \Delta V_N$ becomes large. This means that, far from the magnetopause nose where the magnetosheath flow direction becomes tangential to the magnetopause and makes a right angle with the normal direction to the magnetopause, the net reconnection inflow speed from the magnetosheath side becomes small and then reconnection efficiency reduces gradually. Thus, the magnetic shear angle associated with the occurrence of reconnection is dependent on the magnetopause position. It should be noted that $\Delta V_M / \Delta V_N < (1/R) \tan(\theta/2)$ does not imply the sufficient condition for magnetic reconnection occurrence since the magnetopause boundary shape is not always parabolic (as a zeroth-order approximation) due to possible deformation processes (such as pressure pulses, the Kelvin-Helmholtz instability, and large magnetopause motions). Swisdak et al. (2010) suggested that to promote the reconnection process, the reconnection X-line convection speed should be smaller than the Alfvén speed, $v^* < V_A$. For reconnection occurrence in the presence of shear flows, we suggest that the bulk flow speed ratio $\Delta V_M / \Delta V_N$ should be smaller than the Alfvén speed ratio $\Delta V_{AM} / \Delta V_{AN}$ from equation (8) where ΔV_{AM} and ΔV_{AN} are calculated using B_M and B_N , respectively. We believe that this is the first time to show such a relation between the magnetic shear and the magnetosheath flow streamline vector and this concept could be applied to prediction of the effective extension of the reconnection X-line as depicted with a red dotted curve on the magnetopause in Figure 6. In a future work, we will try to extend our investigation to a larger range of the solar wind-Alfvén Mach number.

Acknowledgments

This work was supported by China-Brazil Joint Laboratory for Space Weather program grant at INPE. We acknowledge NASA contract NAS5-02099 and V. Angelopoulos for use of data from the THEMIS Mission (<http://themis.ssl.berkeley.edu>), specifically C. W. Carlson and J. P. McFadden for use of ESA data, and K. H. Glassmeier, U. Auster, and W. Baumjohann for the use of FGM data provided under the lead of the Technical University of Braunschweig and with financial support through the German Ministry for Economy and Technology and the German Center for Aviation and Space (DLR) under Contract 50 OC 0302. We also acknowledge the OMNIWeb for access to the ACE data (<http://omniweb.gsfc.nasa.gov/>).

References

- Angelopoulos, V. (2008). The THEMIS mission. *Space Science Reviews*, 141(1), 5. <https://doi.org/10.1007/s11214-008-9336-1>
- Auster, H. U., Glassmeier, K. H., Magnes, W., Aydogar, O., Baumjohann, W., Constantinescu, D., et al. (2008). The THEMIS fluxgate magnetometer. *Space Science Reviews*, 141(1), 235–264. <https://doi.org/10.1007/s11214-008-9365-9>
- Borovsky, J. E. (2013). Physical improvements to the solar wind reconnection control function for the Earth's magnetosphere. *Journal of Geophysical Research: Space Physics*, 118, 2113–2121. <https://doi.org/10.1002/jgra.50110>
- Borovsky, J. E., & Birn, J. (2014). The solar wind electric field does not control the dayside reconnection rate. *Journal of Geophysical Research: Space Physics*, 119, 751–760. <https://doi.org/10.1002/2013JA019193>
- Burch, J. L., Moore, T. E., Torbert, R. B., & Giles, B. L. (2016). Magnetospheric multiscale overview and science objectives. *Space Science Reviews*, 199(1), 5–21. <https://doi.org/10.1007/s11214-015-0164-9>
- Cassak, P. A. (2011). Theory and simulations of the scaling of magnetic reconnection with symmetric shear flow. *Physics of Plasmas*, 18(7), 072106. <https://doi.org/10.1063/1.3602859>
- Cassak, P. A., Liu, Y.-H., & Shay, M. (2017). A review of the 0.1 reconnection rate problem. *Journal of Plasma Physics*, 83(5), 715830501. <https://doi.org/10.1017/S0022377817000666>
- Cassak, P. A., & Otto, A. (2011). Scaling of the magnetic reconnection rate with symmetric shear flow. *Physics of Plasmas*, 18(7), 074501. <https://doi.org/10.1063/1.3609771>
- Cassak, P. A., & Shay, M. A. (2007). Scaling of asymmetric magnetic reconnection: General theory and collisional simulations. *Physics of Plasmas*, 14(10), 102114. <https://doi.org/10.1063/1.2795630>
- Dai, L., Wang, C., Angelopoulos, V., & Glassmeier, K.-H. (2015). In situ evidence of breaking the ion frozen-in condition via the non-gyrotropic pressure effect in magnetic reconnection. *Annales Geophysicae*, 33(9), 1147–1153. <https://doi.org/10.5194/angeo-33-1147-2015>
- Deng, X. H., & Matsumoto, H. (2001). Rapid magnetic reconnection in the Earth's magnetosphere mediated by whistler waves. *Nature*, 410, 557–560. <https://doi.org/10.1038/35069018>
- Doss, C. E., Komar, C. M., Cassak, P. A., Wilder, F. D., Eriksson, S., & Drake, J. F. (2015). Asymmetric magnetic reconnection with a flow shear and applications to the magnetopause. *Journal of Geophysical Research: Space Physics*, 120, 7748–7763. <https://doi.org/10.1002/2015JA021489>
- Dungey, J. W. (1961). Interplanetary magnetic field and the auroral zones. *Physical Review Letters*, 6, 47–48. <https://doi.org/10.1103/PhysRevLett.6.47>
- Dunlop, M. W., Zhang, Q.-H., Bogdanova, Y. V., Lockwood, M., Pu, Z., Hasegawa, H., et al. (2011). Extended magnetic reconnection across the dayside magnetopause. *Physical Review Letters*, 107, 025004. <https://doi.org/10.1103/PhysRevLett.107.025004>
- Haaland, S., Runov, A., Artemyev, A., & Angelopoulos, V. (2019). Characteristics of the flank magnetopause: Themis observations. *Journal of Geophysical Research: Space Physics*, 124(5), 3421–3435. <https://doi.org/10.1029/2019JA026459>
- Hietala, H., Phan, T. D., Angelopoulos, V., Oieroset, M., Archer, M. O., Karlsson, T., & Plaschke, F. (2018). In situ observations of a magnetosheath high-speed jet triggering magnetopause reconnection. *Geophysical Research Letters*, 45(4), 1732–1740. <https://doi.org/10.1002/2017GL076525>
- King, J. H., & Papitashvili, N. E. (2005). Solar wind spatial scales in and comparisons of hourly wind and ace plasma and magnetic field data. *Journal of Geophysical Research*, 110, A02104. <https://doi.org/10.1029/2004JA010649>
- La Belle-Hamer, A. L., Otto, A., & Lee, L. C. (1994). Magnetic reconnection in the presence of sheared plasma flow: Intermediate shock formation. *Physics of Plasmas*, 1(3), 706–713. <https://doi.org/10.1063/1.870816>

- La Belle-Hamer, A. L., Otto, A., & Lee, L. C. (1995). Magnetic reconnection in the presence of sheared flow and density asymmetry: Applications to the Earth's magnetopause. *Journal of Geophysical Research*, 100, 11,875–11,889. <https://doi.org/10.1029/94JA00969>
- Liu, Y.-H., Hesse, M., Guo, F., Li, H., & Nakamura, T. K. M. (2018). Strongly localized magnetic reconnection by the super-Alfvénic shear flow. *Physics of Plasmas*, 25(8), 080701. <https://doi.org/10.1063/1.5042539>
- Lopez, R. E., Bruntz, R., Mitchell, E. J., Wilber, M., Lyon, J. G., & Merkin, V. G. (2010). Role of magnetosheath force balance in regulating the dayside reconnection potential. *Journal of Geophysical Research*, 115, A12216. <https://doi.org/10.1029/2009JA014597>
- Ma, X., Otto, A., & Delamere, P. A. (2016). Magnetic reconnection with a fast perpendicular sheared flow. *Journal of Geophysical Research: Space Physics*, 121, 9427–9442. <https://doi.org/10.1002/2016JA023107>
- McFadden, J. P., Carlson, C. W., Larson, D., Ludlam, M., Abiad, R., Elliott, B., et al. (2008). The THEMIS ESA plasma instrument and in-flight calibration. *Space Science Reviews*, 141(1), 277–302. <https://doi.org/10.1007/s11214-008-9440-2>
- Mozer, F. S., Angelopoulos, V., Bonnell, J., Glassmeier, K. H., & McFadden, J. P. (2008). THEMIS observations of modified Hall fields in asymmetric magnetic field reconnection. *Geophysical Research Letters*, 35, L17S04. <https://doi.org/10.1029/2007GL033033>
- Mozer, F. S., Sundkvist, D., McFadden, J. P., Pritchett, P. L., & Roth, I. (2011). Satellite observations of plasma physics near the magnetic field reconnection X line. *Journal of Geophysical Research*, 116, A12224. <https://doi.org/10.1029/2011JA017109>
- Newell, P. T., Sotirelis, T., Liou, K., Meng, C.-I., & Rich, F. J. (2007). A nearly universal solar wind-magnetosphere coupling function inferred from 10 magnetospheric state variables. *Journal of Geophysical Research*, 112, A01206. <https://doi.org/10.1029/2006JA012015>
- Paschmann, G., Papamastorakis, I., Baumjohann, W., Sckopke, N., Carlson, C. W., Sonnerup, B. U. Ö., & Lühr, H. (1986). The magnetopause for large magnetic shear: AMPTE/IRM observations. *Journal of Geophysical Research*, 91, 11,099–11,115. <https://doi.org/10.1029/JA091iA10p11099>
- Paschmann, G., Sonnerup, B. U. Ö., Papamastorakis, I., Sckopke, N., Haerendel, G., Bame, S. J., et al. (1979). Plasma acceleration at the Earth's magnetopause: Evidence for reconnection. *Nature*, 282, 243–246. <https://doi.org/10.1038/282243a0>
- Phan, T. D., Paschmann, G., Gosling, J. T., Oieroset, M., Fujimoto, M., Drake, J. F., & Angelopoulos, V. (2013). The dependence of magnetic reconnection on plasma β and magnetic shear: Evidence from magnetopause observations. *Geophysical Research Letters*, 40, 11–16. <https://doi.org/10.1029/2012GL054528>
- Phan, T. D., Shay, M. A., Gosling, J. T., Fujimoto, M., Drake, J. F., Paschmann, G., et al. (2013). Electron bulk heating in magnetic reconnection at Earth's magnetopause: Dependence on the inflow Alfvén speed and magnetic shear. *Geophysical Research Letters*, 40, 4475–4480. <https://doi.org/10.1002/grl.50917>
- Phan, T. D., Shay, M. A., Haggerty, C. C., Gosling, J. T., Eastwood, J. P., Fujimoto, M., et al. (2016). Ion Larmor radius effects near a reconnection X line at the magnetopause: THEMIS observations and simulation comparison. *Geophysical Research Letters*, 43, 8844–8852. <https://doi.org/10.1002/2016GL070224>
- Pritchett, P. L., Mozer, F. S., & Wilber, M. (2012). Intense perpendicular electric fields associated with three-dimensional magnetic reconnection at the subsolar magnetopause. *Journal of Geophysical Research*, 117, A06212. <https://doi.org/10.1029/2012JA017533>
- Scurry, L., Russell, C. T., & Gosling, J. T. (1994a). Geomagnetic activity and the beta dependence of the dayside reconnection rate. *Journal of Geophysical Research*, 99, 14,811–14,814. <https://doi.org/10.1029/94JA00794>
- Scurry, L., Russell, C. T., & Gosling, J. T. (1994b). A statistical study of accelerated flow events at the dayside magnetopause. *Journal of Geophysical Research*, 99, 14,815–14,829. <https://doi.org/10.1029/94JA00793>
- Shue, J.-H., Chao, J.-K., Song, P., McFadden, J. P., Suvorova, A., Angelopoulos, V., et al. (2009). Anomalous magnetosheath flows and distorted subsolar magnetopause for radial interplanetary magnetic fields. *Geophysical Research Letters*, 36, L18112. <https://doi.org/10.1029/2009GL039842>
- Shue, J.-H., Song, P., Russell, C. T., Steinberg, J. T., Chao, J. K., Zastenker, G., et al. (1998). Magnetopause location under extreme solar wind conditions. *Journal of Geophysical Research*, 103, 17,691–17,700.
- Sonnerup, B., Paschmann, G., Haaland, S., Phan, T., & Eriksson, S. (2016). Reconnection layer bounded by switch-off shocks: Dayside magnetopause crossing by THEMIS D. *Journal of Geophysical Research: Space Physics*, 121, 3310–3332. <https://doi.org/10.1002/2016JA022362>
- Souza, V. M., Gonzalez, W. D., Sibeck, D. G., Koga, D., Walsh, B. M., & Mendes, O. (2017). Comparative study of three reconnection X line models at the Earth's dayside magnetopause using in situ observations. *Journal of Geophysical Research: Space Physics*, 122, 4228–4250. <https://doi.org/10.1002/2016JA023790>
- Swisdak, M., Opher, M., Drake, J. F., & Bibi, F. A. (2010). The vector direction of the interstellar magnetic field outside the heliosphere. *The Astrophysical Journal*, 710(2), 1769–1775. <https://doi.org/10.1088/0004-637x/710/2/1769>
- Swisdak, M., Rogers, B. N., Drake, J. F., & Shay, M. A. (2003). Diamagnetic suppression of component magnetic reconnection at the magnetopause. *Journal of Geophysical Research*, 108(A5), 1218. <https://doi.org/10.1029/2002JA009726>
- Tanaka, K. G., Fujimoto, M., & Shinohara, I. (2010). Physics of magnetopause reconnection: A study of the combined effects of density asymmetry, velocity shear, and guide field. *Geophysical Journal International*, 2010, 202583. <https://doi.org/10.1155/2010/202583>
- Tang, X., Cattell, C., Dombeck, J., Dai, L., Wilson, L. B. III, Breneman, A., & Hupach, A. (2013). THEMIS observations of the magnetopause electron diffusion region: Large amplitude waves and heated electrons. *Geophysical Research Letters*, 40, 2884–2890. <https://doi.org/10.1002/grl.50565>
- Teh, W. L., Eriksson, S., Sonnerup, B. U. Ö., Ergun, R., Angelopoulos, V., Glassmeier, K.-H., et al. (2010). THEMIS observations of a secondary magnetic island within the Hall electromagnetic field region at the magnetopause. *Geophysical Research Letters*, 37, L21102. <https://doi.org/10.1029/2010GL045056>
- Trattner, K. J., Petrinec, S. M., Fuselier, S. A., & Phan, T. D. (2012). The location of reconnection at the magnetopause: Testing the maximum magnetic shear model with THEMIS observations. *Journal of Geophysical Research*, 117, A01201. <https://doi.org/10.1029/2011JA016959>
- Uchino, H., Kurita, S., Harada, Y., Machida, S., & Angelopoulos, V. (2017). Waves in the innermost open boundary layer formed by dayside magnetopause reconnection. *Journal of Geophysical Research: Space Physics*, 122, 3291–3307. <https://doi.org/10.1002/2016JA023300>
- Walsh, B. M., Komar, C. M., & Pfau-Kempf, Y. (2017). Spacecraft measurements constraining the spatial extent of a magnetopause reconnection X line. *Geophysical Research Letters*, 44, 3038–3046. <https://doi.org/10.1002/2017GL073379>
- Walsh, B. M., Phan, T. D., Sibeck, D. G., & Souza, V. M. (2014). The plasmaspheric plume and magnetopause reconnection. *Geophysical Research Letters*, 41, 223–228. <https://doi.org/10.1002/2013GL058802>
- Zhang, Q.-H., Dunlop, M. W., Lockwood, M., Lavraud, B., Bogdanova, Y. V., Hasegawa, H., et al. (2012). Inner plasma structure of the low-latitude reconnection layer. *Journal of Geophysical Research*, 117, A08205. <https://doi.org/10.1029/2012JA017622>
- Zou, Y., Walsh, B. M., Nishimura, Y., Angelopoulos, V., Ruohoniemi, J. M., McWilliams, K. A., & Nishitani, N. (2018). Spreading speed of magnetopause reconnection X-lines using ground-satellite coordination. *Geophysical Research Letters*, 45, 80–89. <https://doi.org/10.1002/2017GL075765>